

Mass of  $^{57}\text{Cu}$ 

C. A. Gagliardi, D. R. Semon, R. E. Tribble, and L. A. Van Ausdeln  
*Cyclotron Institute, Texas A&M University, College Station, Texas 77843*

(Received 28 July 1986)

The ground state  $Q$  value of the reaction  $^{58}\text{Ni}(^7\text{Li}, ^8\text{He})^{57}\text{Cu}$  has been measured and found to be  $-29.613(17)$  MeV. This corresponds to a  $^{57}\text{Cu}$  atomic mass excess of  $-47.303(15)$  MeV. At a beam energy of 76.5 MeV and a scattering angle of  $7^\circ$ , the observed cross section was 17 nb/sr. The implications of these results are discussed.

## I. INTRODUCTION

The shell model predicts that the ground states of  $^{57}\text{Cu}$  and  $^{57}\text{Ni}$  consist of a single nucleon outside a  $^{56}\text{Ni}$  closed core. This simple structure facilitates calculations for these nuclei and increases the importance of precise experimental data regarding them. In particular, knowledge of the masses of the mirror nuclei  $^{57}\text{Cu}$  and  $^{57}\text{Ni}$  may yield important information regarding the Nolen-Schiffer anomaly.<sup>1</sup> The discrepancy between the experimental and theoretical Coulomb displacement energies for similar cases in  $A=17$  and 41 has been attributed<sup>2</sup> to ground state correlations in the nuclear wave functions. It is interesting to examine the mass 57 mirror nuclei to investigate the extension of these systematics to higher  $Z$ . If the  $A=57$  nuclei have true single particle low-lying states, the  $^{57}\text{Cu}$  beta decay rates determine the  $2p_{3/2} \rightarrow 2p_{3/2}$  and  $2p_{3/2} \rightarrow 2p_{1/2}$  Gamow-Teller matrix elements, providing a measure of Gamow-Teller "quenching" in this mass region. On the other hand, matrix elements substantially smaller than one would anticipate for single particle transitions would indicate a breakdown of the simple shell model interpretation of these nuclei. The  $^{57}\text{Cu}$  mass and level structure are also important in calculations of the astrophysical  $rp$  process. Relatively small changes in binding and excitation energies result in significant modifications of the predictions for synthesis of proton-rich isotopes with  $A > 56$  (Ref. 3) and possibly for the time evolution of cosmic x-ray bursts.<sup>4</sup>

$^{57}\text{Cu}$  has been observed in the  $^{57}\text{Cu} \rightarrow ^{57}\text{Ni} + e^+ + \nu_e$  and  $^{58}\text{Ni}(^7\text{Li}, ^8\text{He})^{57}\text{Cu}$  reactions. The former study<sup>5</sup> found the  $^{57}\text{Cu}$  mass excess to be  $-47.34(13)$  MeV and determined its beta decay rates. The latter study<sup>6</sup> determined its mass excess to be  $-47.35(5)$  MeV and identified an excited state at 1.04(4) MeV. We have reinvestigated the  $^{58}\text{Ni}(^7\text{Li}, ^8\text{He})^{57}\text{Cu}$  reaction in order to reduce the uncertainty in the  $^{57}\text{Cu}$  mass excess.

## II. EXPERIMENTAL PROCEDURES AND RESULTS

A 76.5 MeV  $^7\text{Li}^{2+}$  beam from the Texas A&M cyclotron irradiated a target consisting of 1.52 mg/cm<sup>2</sup>  $^{58}\text{Ni}$  (99.98% purity), backed by 1.10 mg/cm<sup>2</sup> of Al. Outgoing ejectiles at 7.0 deg were detected with an Enge split-pole

spectrometer. The beam energy and scattering angle were chosen to permit  $^8\text{He}$ 's from both the  $^{58}\text{Ni}(^7\text{Li}, ^8\text{He})^{57}\text{Cu}$  reaction and the  $^{27}\text{Al}(^7\text{Li}, ^8\text{He})^{26}\text{Si}$  reaction, plus alpha particles from the  $^{27}\text{Al}(^7\text{Li}, \alpha)^{30}\text{Si}$  reaction, to appear on the focal plane simultaneously. The focal plane detector consisted of a 10 cm long resistive wire proportional counter, which provided both position and energy loss measurements, backed by a 1 cm  $\times$  5 cm  $\times$  600  $\mu\text{m}$  thick Si solid state detector. Four parameters were recorded on magnetic tape for each event—position, energy loss through the gas in the wire counter ( $\Delta E$ ), energy deposited in the solid state detector ( $E$ ), and time-of-flight (TOF) relative to the cyclotron rf. Tritons and  $^6\text{He}$ 's were the two most intense particle groups on the counter. In order to minimize deadtime, the  $\Delta E$  and  $E$  thresholds were set above the triton group, and a single channel analyzer set to trigger on the mass 6 group in the TOF spectrum was used as a veto. A 28  $\mu\text{m}$  thick Kapton absorber was inserted between the wire counter and the Si detector to eliminate background due to  $\alpha^+$  and  $^7\text{Li}^{2+}$  particles. With this absorber in place, the TOF spectrum was very clean and provided reliable particle identification. Figure 1 shows a typical TOF spectrum with the  $^8\text{He}$  group clearly identified. The  $\Delta E$  and  $E$  information provided redundant checks against misidentification.

Figure 2 shows typical  $^8\text{He}$  and alpha particle position spectra. The reactions  $^{27}\text{Al}(^7\text{Li}, ^8\text{He})^{26}\text{Si}$  (1.796 MeV) and  $^{27}\text{Al}(^7\text{Li}, \alpha)^{30}\text{Si}$  (g.s., 2.40 MeV) were used for calibration purposes. By using the Ni-Al "sandwich" target, the calibration reactions appeared on the same spectrum as the desired reaction, thereby minimizing the contributions to the uncertainty in the measured  $Q$  value due to changes in the beam energy and the magnetic field in the spectrometer. Data were taken with the target oriented both with the  $^{58}\text{Ni}$  facing the beam and with the Al facing the beam. The change in the observed  $^{27}\text{Al}(^7\text{Li}, \alpha)^{30}\text{Si}$  alpha particle energies in the two orientations provided a precise in-beam determination of the  $^{58}\text{Ni}$  target thickness, which agreed with the thickness determined by weighing to within 5%. This reduced the contribution to the  $Q$ -value uncertainty due to the  $^{58}\text{Ni}$  target thickness to a negligible level. The calibration reactions were also studied with a 1.5 mg/cm<sup>2</sup> Al target. The latter data were analyzed to determine the beam energy and the focal plane calibration.

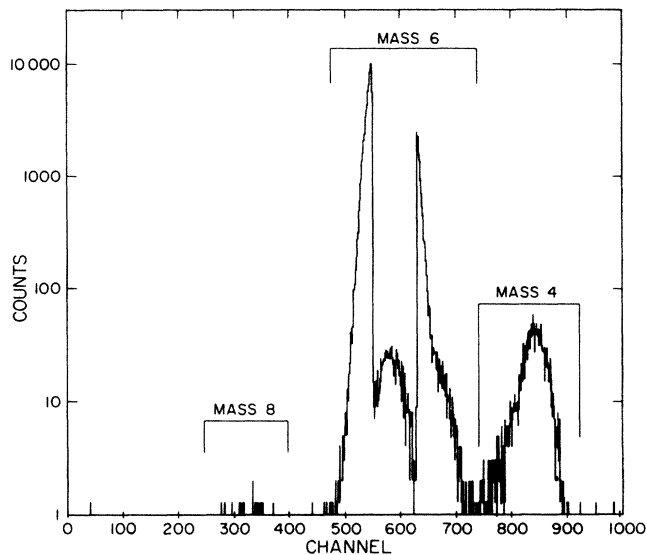


FIG. 1. A typical time-of-flight spectrum used for particle identification. The mass 4, 6, and 8 groups are indicated. The gap in the mass 6 group was caused by the veto discussed in the text. Data taken without the Kapton absorber between the  $\Delta E$  and  $E$  counters included an intense group between the mass 6 and 8 peaks due to  ${}^7\text{Li}^{2+}$ .

The difference in the measured alpha particle energies for the two targets determined the difference in their thicknesses precisely. Only one independent target thickness uncertainty, the average thickness of the two Al targets, contributed to the uncertainty in the measured  $Q$  value. Furthermore, the uncertainty in this target thick-

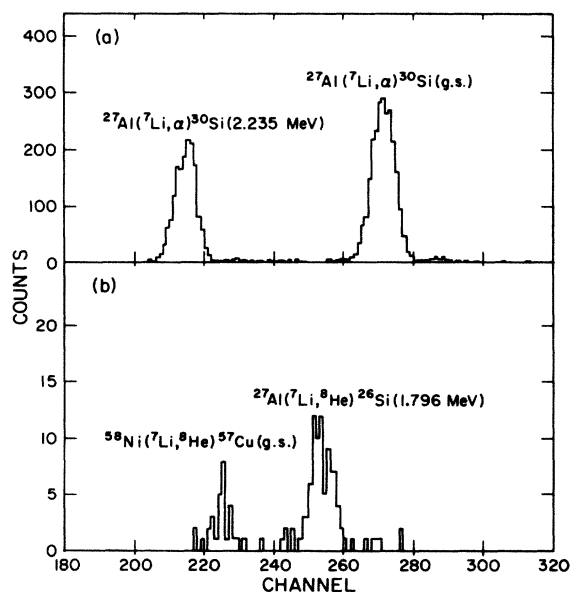


FIG. 2. Spectra (a) and (b) show typical focal plane position spectra after gating on  $\Delta E$ ,  $E$ , and TOF for  $\alpha$  and  ${}^8\text{He}$  particles, respectively. In each case, the observed peaks are identified. These spectra were taken simultaneously with the Ni-Al target described in the text.

ness is equivalent to an uncertainty in the beam energy. Since we used the same reaction for the calibration as for the  $Q$ -value measurement, the  $Q$ -value determination was relatively insensitive to this target thickness.

The  ${}^{58}\text{Ni}({}^7\text{Li},{}^8\text{He}){}^{57}\text{Cu}$   $Q$  value was found to be  $-29.613(17)$  MeV. This corresponds to a  ${}^{57}\text{Cu}$  atomic mass excess of  $-47.303(15)$  MeV. The major contribution to the overall uncertainty was the 12 keV statistical uncertainty in the measured  ${}^8\text{He}$  position centroids. Beam energy, target thickness, scattering angle, and the masses used in calculating the  $Q$  value all made smaller contributions. It should be noted that the present 7 keV uncertainty in our knowledge of the  ${}^8\text{He}$  mass<sup>7</sup> contributed to the uncertainty in the reaction  $Q$  value, but that it dropped out in computing the  ${}^{57}\text{Cu}$  mass excess, since this was done by comparing two different  $({}^7\text{Li},{}^8\text{He})$  reactions. Our result is in excellent agreement with, but more precise than, the previous measurements.<sup>5,6</sup> The agreement between our measured  ${}^{57}\text{Cu}$  mass excess and the previous beta-decay study<sup>5</sup> confirms that the state we observed was the ground state. The measured  $({}^7\text{Li},{}^8\text{He})$  reaction cross sections populating the  ${}^{57}\text{Cu}$  ground state and the  ${}^{26}\text{Si}$  1.796 MeV first excited state were 17 nb/sr and 41 nb/sr, respectively.

### III. DISCUSSION

We compare the present results to several recent mass calculations in Table I. To reduce the systematic differences between the calculations due to different treatments of shell effects, we also present the calculated  $Q_{\text{EC}}$  values. The deviations found for the various models are similar to those found for the other Cu isotopes. In particular, the shell model prediction of Liran and Zeldes and the recursive prediction of Jänecke and Garvey-Kelson are in excellent agreement with the measurements, demonstrating that the  ${}^{57}\text{Cu}$  mass excess is consistent with the systematics in this region. The prediction of Sherrill *et al.*<sup>6</sup> requires special mention. This represents a calculation of

TABLE I. The  ${}^{57}\text{Cu}$  mass excess and  $Q_{\text{EC}}$  are compared to several recent predictions. All energies are in MeV.

Model <sup>a</sup>	Mass excess	$Q_{\text{EC}}$
Myers	-51.47	7.59
Groote-Hilf-Takahashi	-47.73	8.43
Seeger-Howard	-47.7	9.0
Liran-Zeldes	-47.20	8.81
Beiner-Lombard-Mas	-44.9	8.9
Jänecke-Garvey-Kelson	-47.43	8.69
Möller-Nix <sup>b</sup>	-46.42	9.42
Wapstra-Audi <sup>c</sup>	-47.38	8.70
Sherrill <i>et al.</i> <sup>d</sup>		7.87
Experimental result <sup>e</sup>	-47.303(15)	8.774(15)

<sup>a</sup>From Ref. 8 unless otherwise indicated.

<sup>b</sup>Reference 9.

<sup>c</sup>Reference 7.

<sup>d</sup>Reference 6.

<sup>e</sup>This work.

the  $A=57$  Coulomb displacement energy, using radial wave functions obtained in a spherical Hartree-Fock calculation, assuming a closed  $^{56}\text{Ni}$  core, and including the effects of core polarization. The 10% difference between the predicted and measured Coulomb displacement energies is consistent with that found by these calculations<sup>6</sup> throughout the  $f$ - $p$  shell. It has recently been suggested<sup>2</sup> that this anomaly may be explained for the  $A=17$  and 41 single particle nuclei by ground state correlations in the nuclear wave functions. It would be quite interesting to extend these systematics to this higher- $Z$  case to determine whether the anomaly persists or not. If so, it must represent either the influence of additional corrections which have not yet been included in the calculations or the effect of a charge symmetry breaking force.

If we consider the  $^{57}\text{Cu}$  ground state and the  $^{57}\text{Ni}$  low lying states to be pure single particle states, we may combine the measured  $^{57}\text{Cu}$  mass excess with beta decay lifetime measurements<sup>5</sup> to extract  $ft$  values and matrix elements for the corresponding single-particle decays. Following the prescription of Wilkinson and Macefield,<sup>10</sup> we find that the phase space factors are  $f=21432(194)$  and  $10329(108)$  for decays to the  $^{57}\text{Ni}$  ground state and the 1.113 MeV state, respectively. The  $ft$  values are 5187(367) sec and  $65000 \pm_{-21000}^{56000}$  sec. The uncertainties in the two results are dominated by the  $^{57}\text{Cu}$  lifetime and branching ratio uncertainties, respectively. The corresponding Gamow-Teller matrix elements are  $\langle\sigma\rangle=0.35\pm 0.08$  for the  $2p_{3/2}\rightarrow 2p_{3/2}$  transition and  $\langle\sigma\rangle=0.24\pm 0.06$  for the  $2p_{3/2}\rightarrow 2p_{1/2}$  transition, where we have used the formula of Wilkinson,<sup>11</sup> but with updated values for  $g_V$  (Ref. 12) and  $g_A/g_V$  (Ref. 13). Each of these matrix elements is only  $\approx 25\%$  of the corresponding single particle matrix element. This strength reduction is much greater than one would anticipate from the standard Gamow-Teller "quenching" mechanisms. By contrast, the measured matrix elements in the  $A=17$  and 41 cases are 87% and 75% of the single particle values, respectively. This strongly suggests that core excitation plays an important role in the  $A=57$  system. Calculations which explicitly include this degree of freedom are necessary. The impact that this would have on the Coulomb displacement calculations described above is not clear.

The  $^{56}\text{Ni}(p,\gamma)^{57}\text{Cu}$  reaction is an important link in the astrophysical  $rp$  process<sup>3</sup> which may play an important role in the dynamics of collapsing supermassive stars<sup>3</sup> and in the delayed radiation observed following x-ray bursts.<sup>4</sup> The  $rp$  process is the proton analog of the classic  $r$  process. At temperatures of  $T_9=0.2$  to 2 ( $T_9$  is the temperature in units of  $10^9$  K), hydrogen-rich matter burns through a series of  $(p,\gamma)$  and  $(\alpha,p)$  reactions and positron decays, eventually converting He and C-N-O seed nuclei into  $^{56}\text{Ni}$ . At this point, the process stagnates. The long  $^{56}\text{Ni}$  half-life means that heavier nuclei may be formed only after proton capture. The stellar  $^{56}\text{Ni}(p,\gamma)^{57}\text{Cu}$  reaction rate is quite sensitive to the proton resonance energies. Meanwhile, the small reaction  $Q$  value permits  $^{57}\text{Cu}$  photodisintegration to compete favorably with beta decay at relatively low temperatures. The competition between these two effects implies that a relatively narrow temperature window exists for conversion of substantial amounts

of  $^{56}\text{Ni}$  into heavier nuclei. The nuclei which are produced are proton-rich and include a number of extremely rare isotopes, so it is important to understand their yields.

In their studies, Wallace and Woosley<sup>3,4</sup> assumed that the  $^{56}\text{Ni}(p,\gamma)^{57}\text{Cu}$   $Q$  value is 0.691 MeV, and that  $l=1$  and 3 resonances occur at proton energies of 0.422 and 1.752 MeV, respectively. These states would be the analogs of the  $\frac{1}{2}^-$  and  $\frac{5}{2}^-$  states in  $^{57}\text{Ni}$  at 1.113 and 2.443 MeV.<sup>14</sup> The analog of the  $^{57}\text{Ni}$  0.769 MeV  $\frac{5}{2}^-$  state makes a negligible contribution because of the additional angular momentum barrier. Given our new value for the  $^{57}\text{Cu}$  mass excess, we find that the  $^{56}\text{Ni}(p,\gamma)^{57}\text{Cu}$   $Q$  value is 0.690(19) MeV. Sherrill *et al.*<sup>6</sup> chose to treat the  $^{57}\text{Cu}$  excited state which they observed at 1.04(4) MeV as the analog of both the  $\frac{5}{2}^-$  and  $\frac{1}{2}^-$  states for purposes of analysis. This was justified by the fact that the Coulomb displacement energy calculations predict these states to be essentially degenerate. This assumption combined with their more positive  $(p,\gamma)$   $Q$  value implied a substantial reduction in the  $^{56}\text{Ni}(p,\gamma)$  reaction rate for the temperature region of primary interest. In Fig. 3(a), we have recalculated the  $^{56}\text{Ni}(p,\gamma)$  reaction rate as a function of temperature under two different hypotheses. The solid curve assumes that the  $\frac{1}{2}^-$  proton resonance energy is 350 keV, consistent with  $E_x=1.04$  MeV and our revised  $Q$  value. The dashed curve assumes that the state observed previously was, in fact, the  $\frac{5}{2}^-$  state, and that the  $\frac{1}{2}^-$  state is at an excitation energy of 1.11 MeV, as given by Coulomb displacement energy calculations. In both cases, we have included the additional proton resonance at 1.753 MeV from the original  $rp$  calculations. The latter hypothesis essentially reproduces the original results. By contrast, the former hypothesis substantially reduces the  $(p,\gamma)$  reaction rate, especially in the temperature region  $T_9=0.5$  to 0.9. In order to estimate the impact that this change might have upon  $A > 56$  nucleosynthesis, we note that most of the supermassive star models utilized by Wallace

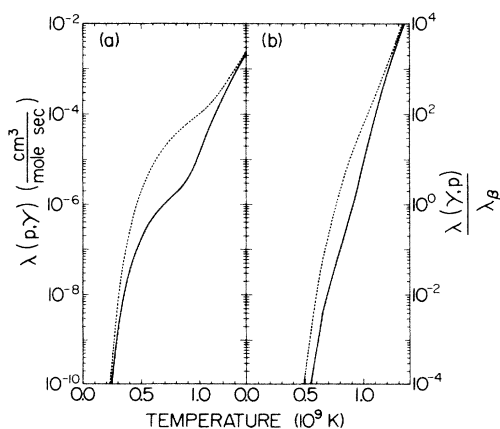


FIG. 3. Panel (a) shows the calculated  $^{56}\text{Ni}(p,\gamma)^{57}\text{Cu}$  reaction rate in  $\text{cm}^3/(\text{mole sec})$ . Panel (b) shows the ratio of the calculated  $^{57}\text{Cu}$  photodisintegration rate to the known beta decay rate. In each case, the solid curve assumes that the  $2p_{1/2}$  proton resonance is at 350 keV and the dashed curve assumes that it is at 420 keV.

and Woosley included hydrogen densities of  $\approx 100 \text{ g/cm}^3$  and characteristic explosion times of 100–1000 sec. Under these conditions, a  $^{56}\text{Ni}(p,\gamma)$  rate of  $10^{-6} \text{ cm}^3/(\text{mole sec})$  would imply a 1–10% proton capture probability. This rate occurs at temperatures of  $T_9=0.47$  and 0.70 with the two hypotheses. In Fig. 3(b), we show the calculated ratio of the  $^{57}\text{Cu}$  photodisintegration rate to its beta-decay rate as a function of temperature, again according to our two hypotheses. When this ratio is much less than 1, essentially all  $^{56}\text{Ni}$  nuclei which capture protons proceed to form heavier isotopes. By contrast, when this ratio is much greater than 1, most  $^{57}\text{Cu}$  which is formed returns to  $^{56}\text{Ni}$  via photodisintegration. This quantity is primarily determined by the  $^{56}\text{Ni}(p,\gamma)^{57}\text{Cu}$   $Q$  value, so the difference between the two hypotheses is not great in this case. The critical temperature when  $\lambda_{(p,\gamma)}/\lambda_\beta=1$  shifts from  $T_9=0.77$  to 0.92 under the two hypotheses. We see that substantial heavy element synthesis will occur at different temperatures, depending upon the actual excitation energy of the  $^{57}\text{Cu}$   $\frac{1}{2}^-$  state. Clearly, more detailed spectroscopic information is needed.

Finally, it should be noted that our measured ( $^7\text{Li},^8\text{He}$ ) cross section at 76.5 MeV was only  $\approx 13\%$  of that found<sup>6</sup> in the same reaction at 174 MeV. If this exotic reaction is to be used in further mass measurements, there is a sub-

stantial advantage to be gained by running at higher beam energies.

#### IV. CONCLUSIONS

We have remeasured the  $Q$  value of the  $^{58}\text{Ni}(^7\text{Li},^8\text{He})^{57}\text{Cu}$  reaction, and from this, we have deduced the  $^{57}\text{Cu}$  mass excess. Our results are in excellent agreement with, but substantially more precise than, the previous measurements. The  $^{57}\text{Cu}$  mass is consistent with the systematics for this region. In particular, the experimental  $A=57$  Coulomb displacement energy is  $\approx 10\%$  larger than predicted<sup>6</sup> by a detailed Hartree-Fock calculation. This discrepancy indicates either that important nuclear effects have been neglected in the calculation or that a charge symmetry breaking force may be present. The  $^{57}\text{Cu}$  Gamow-Teller matrix elements suggest that the  $A=57$  nuclear wave functions include substantial multiparticle, multihole components. More detailed spectroscopic information for  $^{57}\text{Cu}$  is required before the importance of the  $rp$  process in heavy element synthesis may be determined.

This work was supported in part by the U.S. Department of Energy and by the Robert A. Welch Foundation.

<sup>1</sup>J. A. Nolen and J. P. Schiffer, Phys. Lett. **29B**, 396 (1969).

<sup>2</sup>S. Shlomo (unpublished).

<sup>3</sup>R. K. Wallace and S. E. Woosley, Astrophys. J. Suppl. **45**, 389 (1981).

<sup>4</sup>R. K. Wallace and S. E. Woosley, in *High Energy Transients in Astrophysics*, Proceedings of the Conference on High Energy Transients in Astrophysics, Santa Cruz, AIP Conf. Proc. No. 115, edited by S. E. Woosley (AIP, New York, 1984), p. 319.

<sup>5</sup>T. Shinozuka *et al.*, Phys. Rev. C **30**, 2111 (1984).

<sup>6</sup>B. Sherrill *et al.*, Phys. Rev. C **31**, 875 (1985).

<sup>7</sup>A. H. Wapstra and G. Audi, Nucl. Phys. **A432**, 1 (1985).

<sup>8</sup>S. Maripuu (special editor), At. Data Nucl. Data Tables **17**, 411 (1976).

<sup>9</sup>P. Möller and J. R. Nix, At. Data Nucl. Data Tables **26**, 165 (1981).

<sup>10</sup>D. H. Wilkinson and B. E. F. Macefield, Nucl. Phys. **A232**, 58 (1974).

<sup>11</sup>D. H. Wilkinson, Nucl. Phys. **A209**, 470 (1973).

<sup>12</sup>D. H. Wilkinson, Nucl. Phys. **A377**, 474 (1982).

<sup>13</sup>P. Bopp *et al.*, Phys. Rev. Lett. **56**, 919 (1986).

<sup>14</sup>T. W. Burrows and M. R. Bhat, Nucl. Data Sheets **47**, 1 (1986).